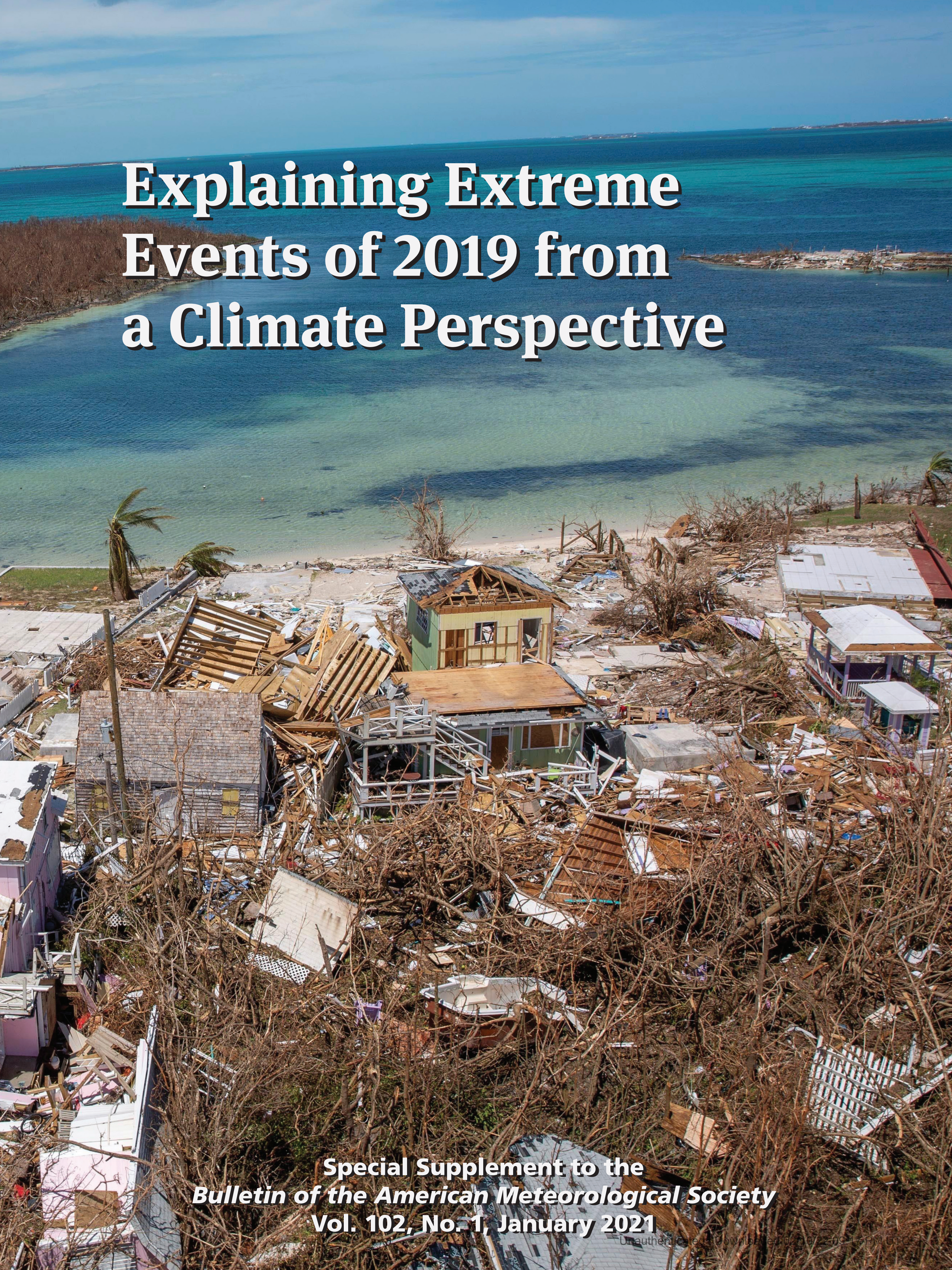

Explaining Extreme Events of 2019 from a Climate Perspective

Special Supplement to the
Bulletin of the American Meteorological Society
Vol. 102, No. 1, January 2021

EXPLAINING EXTREME EVENTS OF 2019 FROM A CLIMATE PERSPECTIVE

Editors

Stephanie C. Herring, Nikolaos Christidis, Andrew Hoell,
Martin P. Hoerling, and Peter A. Stott

***BAMS* Special Editors for Climate**

Andrew King, Thomas Knutson,
John Nielsen-Gammon, and Friederike Otto

Special Supplement to the

Bulletin of the American Meteorological Society

Vol. 102, No. 1, January 2021

American Meteorological Society

Corresponding Editor:

Stephanie C. Herring, Ph.D.
NOAA National Centers for Environmental Information
325 Broadway, E/CC23, Rm 1B-131
Boulder, CO 80305-3328
E-mail: stephanie.herring@noaa.gov

Cover: Ruins and rubble are all that are left of homes destroyed by Hurricane Dorian viewed from a U.S. Customs and Border Protection rescue helicopter 5 September 2019 in Marsh Harbour, Abaco, Bahamas. Dorian struck the small island nation as a Category 5 storm with winds of 185 mph. (credit: Planetpix/Alamy Stock Photo)

HOW TO CITE THIS DOCUMENT

Citing the complete report:

Herring, S. C., N. Christidis, A. Hoell, M. P. Hoerling, and P. A. Stott, Eds., 2021: Explaining Extreme Events of 2019 from a Climate Perspective. *Bull. Amer. Meteor. Soc.*, **102** (1), S1–S112, https:/doi.org/10.1175/BAMS-ExplainingExtremeEvents2019.1.

Citing a section (example):

Amaya, D. J., M. A. Alexander, A. Capotondi, C. Deser, K. B. Karnauskas, A. J. Miller, and N. J. Mantua, 2021: Are Long-Term Changes in Mixed Layer Depth Influencing North Pacific Marine Heatwaves? [in "Explaining Extremes of 2019 from a Climate Perspective"]. *Bull. Amer. Meteor. Soc.*, **102** (1), S59–S66, doi:https://doi.org/10.1175/BAMS-D-20-0144.1.

TABLE OF CONTENTS

1. Increased Risk of the 2019 Alaskan July Fires due to Anthropogenic Activity S1
2. Anthropogenic Influence on Hurricane Dorian's Extreme Rainfall S9
3. Quantifying Human-Induced Dynamic and Thermodynamic Contributions to Severe Cold Outbreaks Like November 2019 in the Eastern United States S17
4. Anthropogenic Influences on Extreme Annual Streamflow into Chesapeake Bay from the Susquehanna River S25
5. Anthropogenic Contribution to the Rainfall Associated with the 2019 Ottawa River Flood S33
6. Extremely Warm Days in the United Kingdom in Winter 2018/19 . . . . S39
7. CMIP6 Model-Based Assessment of Anthropogenic Influence on the Long Sustained Western Cape Drought over 2015–19 . . . . S45
8. Has Global Warming Contributed to the Largest Number of Typhoons Affecting South Korea in September 2019? S51
9. Are Long-Term Changes in Mixed Layer Depth Influencing North Pacific Marine Heatwaves? S59
10. Was the Extended Rainy Winter 2018/19 over the Middle and Lower Reaches of the Yangtze River Driven by Anthropogenic Forcing? S67
11. Roles of Anthropogenic Forcing and Natural Variability in the Record-Breaking Low Sunshine Event in January–February 2019 over the Middle-Lower Yangtze Plain S75
12. Attribution of the Extreme Drought-Related Risk of Wildfires in Spring 2019 over Southwest China S83
13. Attribution of 2019 Extreme Spring-Early Summer Hot Drought over Yunnan in Southwestern China S91
14. Anthropogenic Influence on 2019 May–June Extremely Low Precipitation in Southwestern China S97
15. Anthropogenic Influences on Heavy Precipitation during the 2019 Extremely Wet Rainy Season in Southern China S103

Anthropogenic Influence on Hurricane Dorian's Extreme Rainfall

Kevin A. Reed, Michael F. Wehner, Alyssa M. Stansfield, and Colin M. Zarzycki

Hindcast attribution simulations suggest that anthropogenic climate change increased the likelihood of Hurricane Dorian's extreme 3-hourly rainfall amounts and total accumulated rainfall by 8%–18% and 5%–10%, respectively.

AFFILIATIONS: Reed and Stansfield—School of Marine and Atmospheric Sciences, Stony Brook University, Stony Brook, New York; **Wehner**—Lawrence Berkeley National Laboratory, Berkeley, California; **Zarzycki**—Pennsylvania State University, State College, Pennsylvania

CORRESPONDING AUTHOR: Kevin Reed, kevin.reed@stonybrook.edu

DOI:10.1175/BAMS-D-20-0160.1

A supplement to this article is available online (10.1175/BAMS-D-20-0160.2)

Hurricane Dorian formed on 24 August 2019 from a tropical wave and developed into a Category 5 hurricane on 1 September 2019 before making landfall in the Bahamas (Avila et al. 2020). The impacts on the Bahamas were extreme, including rainfall totals over 0.5 m in the region (Avila et al. 2020). This was on the heels of the recent damaging North Atlantic hurricanes of 2017 and 2018, which impacted various regions with different combinations of hazards (Klotzbach et al. 2018a; Avila 2019).

Tropical cyclones are very costly natural disasters (Klotzbach et al. 2018b) due to a diverse set of impacts, including high winds, extreme rainfall, storm surge, and fresh and/or saltwater flooding. Previous work has explored the potential impact of climate change, both in the past and projected into the future, on these hazards (e.g., Knutson et al. 2010, 2019, 2020; Christensen et al. 2013; Walsh et al. 2016). A recent review by Knutson et al.

(2020) estimates that the global mean near-storm rainfall increases at about 7% per 1°C. Significant advances have been made in attribution frameworks to help quantify the effect of climate change on individual hurricanes. Investigations of individual storms using various attribution methodologies suggest that changes in rainfall can exceed the Knutson et al. (2020) estimate, although there are uncertainties associated with the use of different rainfall metrics (e.g., Risser and Wehner 2017; van Oldenborgh et al. 2017; Emanuel 2017; Wang et al. 2018; Keellings and Hernández Ayala 2019). Here we apply a hindcast attribution methodology to Hurricane Dorian previously developed and tested for Hurricane Florence (Reed et al. 2020), Typhoon Haiyan (Wehner et al. 2019), and numerous other tropical cyclones (Patricola and Wehner 2018) that focuses on storm rainfall due to confidence in the model's ability to simulate precipitation processes.

Methods.

This work makes use of the variable-resolution configuration of the Community Atmosphere Model version 5 (CAM5; Neale et al. 2012) with a 28-km nest over the North Atlantic [as in Reed et al. (2020)]. CAM5, at grid spacings of 28 km, has been used previously to explore tropical cyclones and rainfall at both climate (e.g., Wehner et al. 2014; Zarzycki and Jablonowski 2014; Wehner et al. 2015; Bacmeister et al. 2018; Stansfield et al. 2020a) and weather time scales (e.g., Zarzycki and Jablonowski 2015; Wehner et al. 2019; Reed et al. 2020). Following the methodology of Zarzycki and Jablonowski (2015), short 7-day ensemble hindcasts are initialized both in advance of and after Hurricane Dorian's landfall in the Bahamas at 12-h increments starting at 1200 UTC 30 August and ending at 0000 UTC 4 September for a total of 10 initialization times. The CAM5 hindcasts are initialized with atmospheric and ocean surface analyses from NOAA's GDAS and OISST, respectively, to construct an ensemble under the "actual" climate and weather conditions. Twenty ensemble members are created at each initialization time by perturbing a set of three parameters (convective time scale, precipitation coefficient, and parcel fractional mass entrainment rate) in the Zhang and McFarlane (1995) deep convection parameterization [following Reed et al. (2020), who used the parameter ranges from He and Posselt (2015)], resulting in a 200-member ensemble. Note that since modifying parameters in the convective parameterization can modulate precipitation (e.g., Zhao et al. 2012) the ensembles are perturbed with the same values on a member-to-member basis across all experiments.

A "counterfactual" ensemble (20 members at each initialization time) is constructed by removing the anthropogenic signal from the 3D air temperature, 3D specific humidity, and 2D sea surface temperature (SST) initial conditions used for the actual ensemble. Following Reed et al. (2020), the anthropogenic signal is approximated by computing the difference between the All-Hist (with prescribed SST, sea ice, greenhouse gases, and aerosols derived from observations) and Nat-Hist (with prescribed SST, surface ice, greenhouse gases, and aerosols boundary conditions modified to remove anthropogenic forcings) CAM5 simulations completed under Climate of the Twentieth Century (C20C+) Detection and Attribution Project protocols (available at portal.nersc.gov/c20c), designed for event attribution (Stone et al. 2019), for the average of August and September for the last 20 years (1996–2016). This results in a difference of SST of about 0.75°C in the Bahamas region. Dynamical fields, such as zonal and meridional wind, are not adjusted in the initial conditions counterfactual ensemble, consistent with Reed et al. (2020).

For both the actual and counterfactual ensembles, the TempestExtremes software package (Ullrich and Zarzycki 2017) is used to detect and track the simulated storms and extract storm-related rainfall using the approach of Stansfield et al. (2020b), which specifies storm rainfall to be within an outer radius defined by a 8 m s^{-1} threshold of the azimuthally averaged azimuthal wind speed. Hurricane Dorian's observed rainfall estimates from NASA's Integrated Multi-satellitE Retrievals for GPM (IMERG; https://pmm.nasa.gov/data-access/downloads/gpm) are used to calculate the maximum 3-hourly rainfall amount, while recognizing that there are substantial uncertainties associated with heavy tropical cyclone rainfall in satellite estimates (e.g., underestimating storm rainfall over land; Chen et al. 2013).

Given resolution limitations, this work focuses on characterizing changes in the precipitation associated with Hurricane Dorian in the CAM5 hindcasts simulations. It is well known that intensity can influence storm rainfall and that numerical simulations at these grid spacings are limited in their ability to represent intensity (i.e., maximum surface wind; Davis et al. 2018). Furthermore, the work of Patricola and Wehner (2018) demonstrated, using a comparable hindcast attribution framework with the Weather Research and Forecasting (WRF) Model, that while the simulated intensity (i.e., maximum wind speed) of hurricanes is underestimated at 27-km grid spacing compared to 3-km grid spacing, changes in storm rainfall due to warming are relatively insensitive to this resolution difference. The CAM5 actual ensemble simulates an average intensity bias at a lead time of 72 h (120 h) of approximately 47 hPa (39 hPa), which is comparable to the intensity errors for the 27-km grid spacing simulation of other category 5 hurricanes in Patricola and Wehner (2018) and consistent with other operational numerical weather prediction for an intensifying major hurricane. While imperfect, CAM5 hindcasts of tropical cyclones have demonstrated skill in representing storm rainfall (Reed et al. 2020) and tracks comparable to forecasts from operational numerical weather prediction (Zarzycki and Jablonowski 2015).

Results.

Comparing 3-hourly rainfall amounts and total accumulated rainfall across the actual and counterfactual ensembles allows for an analysis of the potential impact of observed climate change on Hurricane Dorian. The ensemble mean accumulated precipitation throughout the lifetime of the simulated storms at all initialization times is shown in Fig. 1. The spatial ensemble mean rainfall patterns suggest that there are similarities in the simulated tracks for the actual and counterfactual ensembles for a given initialization time, allowing for direct comparison. However, there are variations in the simulated tracks across different initialization times (Fig. ES1), consistent with real-time operational forecasts. Furthermore, additional analysis shows that the average CAM5 hindcast track error at a lead time of 72 h (120 h) is 144 km (230 km), which is within range of track errors associated with the official operational models used by the National Hurricane Center. When comparing the magnitude of the ensemble mean accumulated rainfall at individual initialization times between the actual and counterfactual ensembles, Fig. 1 indicates that many areas experience increased precipitation in the actual ensemble compared to the counterfactual. This is also true in the region near the Bahamas (defined to be 25.5°–29.5°N, 76°–80°W; outlined in Fig. 1) where the most extreme rainfall accumulations were observed to occur (Fig. ES2), providing some evidence that the model represents extreme rainfall sufficiently well in the region. The Bahamas region is simulated to experience the highest rainfall accumulations in the ensembles during the initializations between 0000 UTC 31 August and 1200 UTC 2 September.

Figure 2a shows the probability distribution of the 3-hourly rainfall amounts associated with the simulated storm over its lifetime for all ensembles. The results suggest that there is a shift toward higher 3-hourly rainfall amounts in the actual ensemble with climate change. The likelihood of 3-hourly precipitation above the IMERG estimated maximum of 0.136 m increases from approximately 0.145% in the counterfactual ensemble to about 0.168% in the actual ensemble, representing an increase of 16% (95% confidence interval: 14%–18%) in the likelihood of such events. It is worth noting that a Dorian-like storm with rainfall at or above the IMERG estimated 3-hourly maximum is a 99.8th percentile event across the 200-member CAM5 ensemble, which is indeed a rare event at the tail of the simulated distribution, suggesting that the model framework has some skill in reproducing the extreme rainfall rates observed for Hurri-

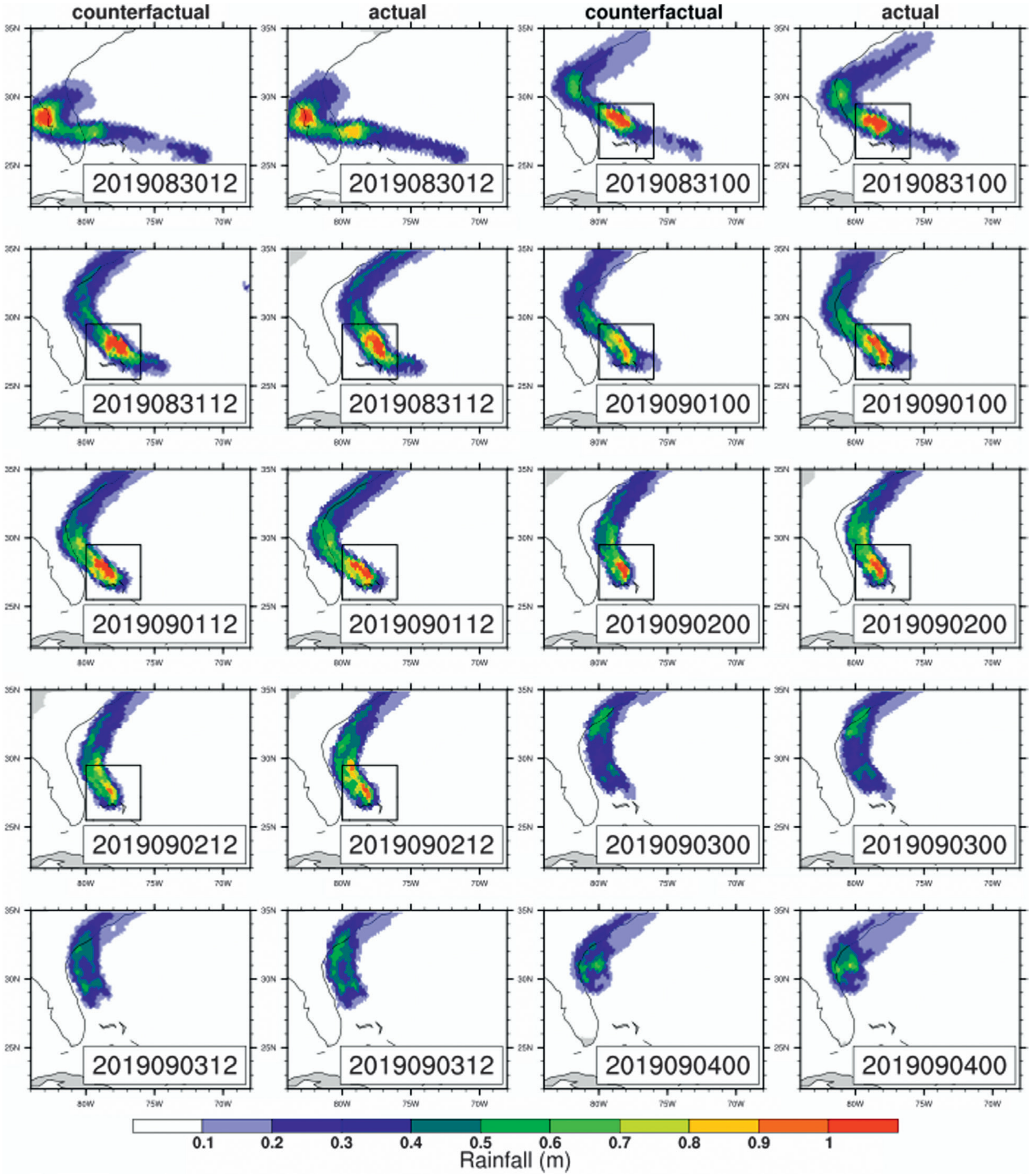

Fig. 1. Total accumulated ensemble mean storm-related rainfall (m) over the entire forecast period (excluding the first 12 h) for each initialization time (as labeled) of the counterfactual and actual realizations of Hurricane Dorian. Each initialization time contains 20 ensemble members. The Bahamas region is denoted (black outline) for the initialization times used for the region-specific analysis.

cane Dorian. Given that the IMERG maximum is an estimate, we performed a sensitivity analysis by repeating the calculation for a maximum 3-hourly rainfall amount of 0.1 and 0.17 m (representing a ±25% change from the estimated maximum), and the percentage increase ranges from 8% to 13% in the likelihood of such events. Analysis of the maximum 3-hourly rainfall amounts (Fig. 2c) in each ensemble reveals an increase in the maximum precipitation of 2% (95% confidence interval: –1% to 4%). Figure 2b shows the same probability distribution but for the Bahamas region (outlined in Fig. 1) associated with the initialization times that produce large rainfall amounts in the region. The results again suggest that there is a shift toward higher 3-hourly rainfall amounts in the actual ensemble with climate change, particularly at the highest rain rates. The maximum 3-hourly rainfall in the Bahamas region (Fig. 2d) is simulated to have increased by 2% (95% confidence interval: 1%–3%) due to climate change, while the likelihood of 0.136 m amounts increases marginally (<1%).

A more integrated measure of rainfall associated with Hurricane Dorian is the sum of all accumulated precipitation during the simulated storms, in which CAM5 demonstrates some skill in reproducing the accumulated amounts and spatial distribution (Fig. 1) when compared to IMERG estimates (Fig. ES2). For the full ensemble there is a clear increase in the total accumulated precipitation of 7% (95% confidence interval: 5% to 10%) and in the subset ensemble in the Bahamas region of 3% (95% confidence interval: –1% to 7%). Note that for all analysis in this section the 95% confidence interval is derived from a bootstrap analysis of 1000 samples.

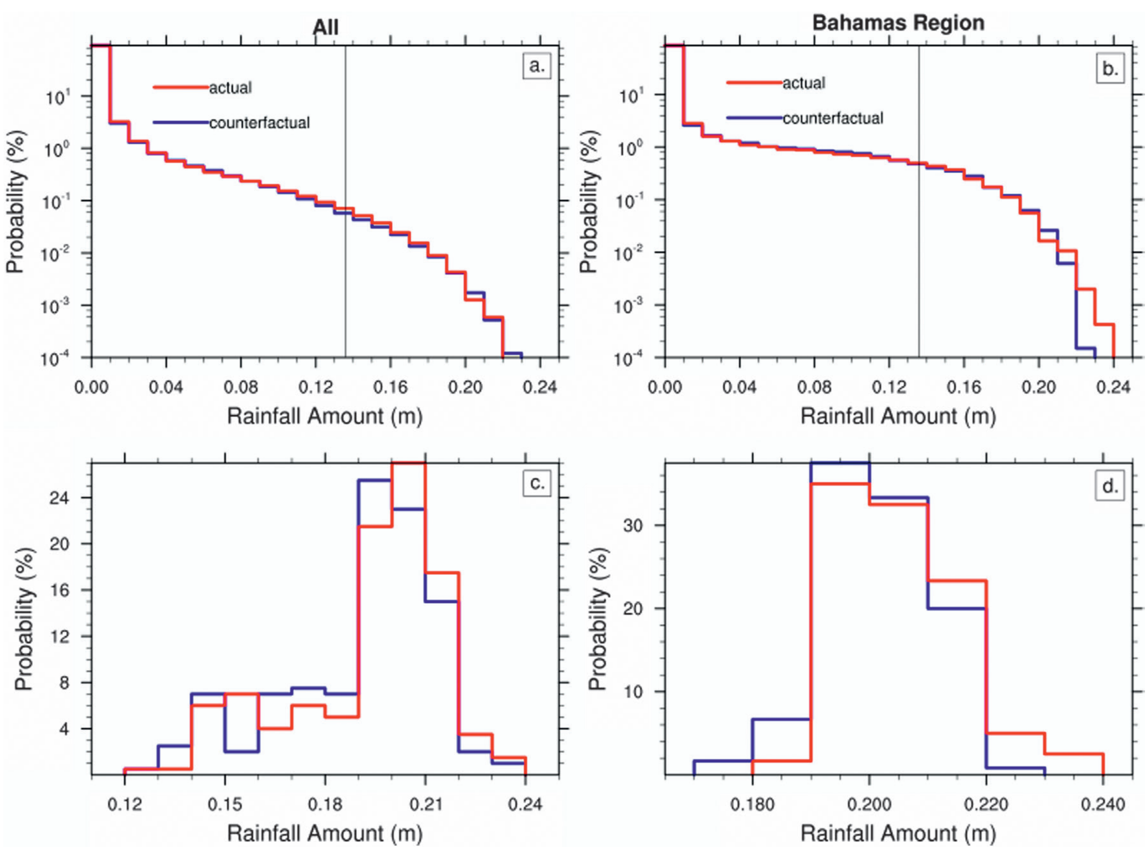

Fig. 2. Probability distributions of the (a),(b) 3-hourly rainfall amounts and (c),(d) maximum 3-hourly rainfall amounts associated with Hurricane Dorian in the actual and counterfactual ensembles. Results are shown for (left) rainfall at all initialization times throughout the domain and (right) the six subset initialization times and Bahamas region only (see Fig. 1). The vertical line in (a),(b) represents observed maximum 3-hourly rainfall amount as estimated by IMERG.

Conclusions.

The work explores the potential impact of climate change on the rainfall associated with Hurricane Dorian using the CAM5 hindcast attribution framework. The analysis indicates the likelihood of 3-hourly rainfall accumulations above 0.136 m (observed) increases by 16%, while the maximum 3-hourly rainfall amount increases by 2% due to climate change. When focusing on the extreme accumulations of rainfall that occurred over multiple days, the analysis reveals the total accumulated rainfall over the area of the simulated storm increased by 7%. This work provides additional evidence that climate change has increased the magnitude and probability of extreme rainfall associated with recent devastating hurricanes (Risser and Wehner 2017; van Oldenborgh et al. 2017; Emanuel 2017; Wang et al. 2018; Trenberth et al. 2018; Keellings and Hernández Ayala 2019; Reed et al. 2020) and is consistent with projected changes in tropical cyclone–related precipitation under future climate change scenarios (e.g., Villarini et al. 2014; Knutson et al. 2020; Stansfield et al. 2020a). Depending on the rainfall metric used the simulated change presented here for Hurricane Dorian is closer to, or below, the theoretical Clausius–Clapeyron scaling of ~4% to 6% (given the 0.75°C SST change). However, differences in metrics and methodologies, including sensitivities to model resolution which will be the focus of future work, among the various hurricane precipitation attribution studies are critical to the interpretation of these numbers. As global SSTs continue to warm, rainfall accumulations associated with storms like Hurricane Dorian will undoubtedly continue to increase.

Acknowledgments. This work was partially supported by the Stony Brook Foundation's Minghua Zhang Early Career Faculty Innovation Fund, NASA under Grant 80NSSC19K0717, the NSF Research Traineeship (NRT) program (1633299), and the Regional and Global Model Analysis (RGMA) program area of the DOE's Office of Science under Contract DE-AC02-05CH11231.

References

Avila, L. A., 2019: The 2018 Atlantic hurricane season: Another catastrophic year for the United States. *Weatherwise*, **72**, 14–21, https://doi.org/10.1080/00431672.2019.1612201.

——, S. R. Stewart, R. Berg, and A. B. Hagen, 2020: National Hurricane Center Tropical Cyclone Report, Tropical Cyclone Report Hurricane Dorian AL052019, National Hurricane Center, 74 pp., https://www.nhc.noaa.gov/data/tcr/AL052019_Dorian.pdf.

Bacmeister, J. T., K. A. Reed, C. Hannay, P. J. Lawrence, S. C. Bates, J. E. Truesdale, N. A. Rosenbloom, and M. N. Levy, 2018: Projected changes in tropical cyclone activity under future warming scenarios using a high-resolution climate model. *Climatic Change*, **146**, 547–560, https://doi.org/10.1007/s10584-016-1750-x.

Chen, Y., E. E. Ebert, K. J. E. Walsh, and N. E. Davidson, 2013: Evaluation of TRMM 3B42 precipitation estimates of tropical cyclone rainfall using PACRAIN data. *J. Geophys. Res. Atmos.*, **118**, 2184–2196, https://doi.org/10.1002/jgrd.50250.

Christensen, J. H., and Coauthors, 2013: Climate phenomena and their relevance for future regional climate change. Climate Change 2013: The Physical Science Basis, T. F. Stocker et al., Eds., Cambridge University Press, 1217–1308.

Davis, C. A., 2018: Resolving tropical cyclone intensity in models. *Geophys. Res. Lett.*, **45**, 2082–2087. https://doi.org/10.1002/2017GL076966.

Emanuel, K., 2017: Assessing the present and future probability of Hurricane Harvey's rainfall. *Proc. Natl. Acad. Sci. USA*, **114**, 12 681–12 684, https://doi.org/10.1073/pnas.1716222114.

He, F., and D. J. Posselt, 2015: Impact of parameterized physical processes on simulated tropical cyclone characteristics in the Community Atmosphere Model. *J. Climate*, **28**, 9857–9872, https://doi.org/10.1175/JCLI-D-15-0255.1.

Keellings, D., and J. J. Hernández Ayala, 2019: Extreme rainfall associated with Hurricane Maria over Puerto Rico and its connections to climate variability and change. *Geophys. Res. Lett.*, **46**, 2964–2973, https://doi.org/10.1029/2019GL082077.

Klotzbach, P. J., C. J. Schreck III, J. M. Collins, M. M. Bell, E. S. Blake, and D. Roache, 2018a: The extremely active 2017 North Atlantic hurricane season. *Mon. Wea. Rev.*, **146**, 3425–3443, https://doi.org/10.1175/MWR-D-18-0078.1.

——, S. G. Bowen, R. Pielke, and M. Bell, 2018b: Continental U.S. hurricane landfall frequency and associated damage: Observations and future risks. *Bull. Amer. Meteor. Soc.*, **99**, 1359–1376, https://doi.org/10.1175/BAMS-D-17-0184.1.

Knutson, T. R., and Coauthors, 2010: Tropical cyclones and climate change. *Nat. Geosci.*, **3**, 157–163, https://doi.org/10.1038/ngeo779.

——, and Coauthors, 2019: Tropical cyclones and climate change assessment: Part I. Detection and attribution. *Bull. Amer. Meteor. Soc.*, **100**, 1987–2007, https://doi.org/10.1175/BAMS-D-18-0189.1.

——, and Coauthors, 2020: Tropical cyclones and climate change assessment: Part II. Projected response to anthropogenic warming. *Bull. Amer. Meteor. Soc.*, **101**, E303–E322, https://doi.org/10.1175/BAMS-D-18-0194.1.

Neale, R. B., C. C. Chen, A. Gettelman, P. H. Lauritzen, S. Park, D. L. Williamson, and M. A. Taylor, 2012: Description of the NCAR Community Atmosphere Model (CAM 5.0). NCAR Tech. Note NCAR/TN-486+STR, 274 pp., www.cesm.ucar.edu/models/cesm1.0/cam/docs/description/cam5_desc.pdf.

Patricola, C. M., and M. F. Wehner, 2018: Anthropogenic influences on major tropical cyclone events. *Nature*, **563**, 339–346, https://doi.org/10.1038/s41586-018-0673-2.

Reed, K. A., A. M. Stansfield, M. F. Wehner, and C. M. Zarzycki, 2020: Forecasted attribution of the human influence on Hurricane Florence. *Sci. Adv.*, **6**, eaaw9253, https://doi.org/10.1126/sciadv.aaw9253.

Risser, M. D., and M. F. Wehner, 2017: Attributable human-induced changes in the likelihood and magnitude of the observed extreme precipitation during Hurricane Harvey. *Geophys. Res. Lett.*, **44**, 12 457–12 464, https://doi.org/10.1002/2017GL075888.

Stansfield, A. M., K. A. Reed, and C. M. Zarzycki, 2020a: Changes in precipitation from North Atlantic tropical cyclones under RCP scenarios in the variable-resolution Community Atmosphere Model. *Geophys. Res. Lett.*, **47**, e2019GL086930, https://doi.org/10.1029/2019GL086930.

——, ——, ——, P. A. Ullrich, and D. R. Chavas, 2020b: Assessing tropical cyclones' contribution to precipitation over the eastern United States and sensitivity to the variable-resolution domain extent. *J. Hydrometeor.*, **21**, 1425–1445, https://doi.org/10.1175/JHM-D-19-0240.1.

Stone, D. A., and Coauthors, 2019: Experiment design of the International CLIVAR C20C+ detection and attribution project. *Wea. Climate Extrem.*, **24**, 100206, https://doi.org/10.1016/j.wace.2019.100206.

Trenberth, K. E., L. Cheng, P. Jacobs, Y. Zhang, and J. Fasullo, 2018: Hurricane Harvey links to ocean heat content and climate change adaptation. *Earth's Future*, **6**, 730–744, https://doi.org/10.1029/2018EF000825.

Ullrich, P. A., and C. M. Zarzycki, 2017: TempestExtremes: A framework for scale-insensitive pointwise feature tracking on unstructured grids. *Geosci. Model Dev.*, **10**, 1069–1090, https://doi.org/10.5194/gmd-10-1069-2017.

van Oldenborgh, G. J., and Coauthors, 2017: Attribution of extreme rainfall from Hurricane Harvey, August 2017. *Environ. Res. Lett.*, **12**, 124009, https://doi.org/10.1088/1748-9326/aa9ef2.

Villarini, G., D. A. Lavers, E. Scoccimarro, M. Zhao, M. F. Wehner, G. A. Vecchi, T. R. Knutson, and K. A. Reed, 2014: Sensitivity of tropical cyclone rainfall to idealized global scale forcings. *J. Climate*, **27**, 4622–4641, https://doi.org/10.1175/JCLI-D-13-00780.1.

Walsh, K. J., and Coauthors, 2016: Tropical cyclones and climate change. *Wiley Interdiscip. Rev.: Climate Change*, **7**, 65–89, https://doi.org/10.1002/WCC.371.

Wang, S.-Y. S., L. Zhao, J.-H. Yoon, P. Klotzbach, and R. R. Gillies, 2018: Quantitative attribution of climate effects on Hurricane Harvey's extreme rainfall in Texas. *Environ. Res. Lett.*, **13**, 054014, https://doi.org/10.1088/1748-9326/aabb85.

Wehner, M., and Coauthors, 2014: The effect of horizontal resolution on simulation quality in the Community Atmospheric Model, CAM5.1. *J. Adv. Model. Earth Syst.*, **6**, 980–997, https://doi.org/10.1002/2013MS000276.

——, K. A. Reed, D. Stone, W. D. Collins, and J. Bacmeister, 2015: Resolution dependence of future tropical cyclone projections of CAM5.1 in the U.S. CLIVAR hurricane working group idealized configurations. *J. Climate*, **28**, 3905–3925, https://doi.org/10.1175/JCLI-D-14-00311.1.

——, C. Zarzycki, and C. Patricola, 2019: Estimating the human influence on tropical cyclone intensity as the climate changes. Hurricane Risk, Vol. I, J. Collins and K. Walsh, Eds., Springer, 235–260.

Zarzycki, C. M., and C. Jablonowski, 2014: A multidecadal simulation of Atlantic tropical cyclones using a variable-resolution global atmospheric general circulation model. *J. Adv. Model. Earth Syst.*, **6**, 805–828, https://doi.org/10.1002/2014MS000352.

——, and ——, 2015: Experimental tropical cyclone forecasts using a variable-resolution global model. *Mon. Wea. Rev.*, **143**, 4012–4037, https://doi.org/10.1175/MWR-D-15-0159.1.

Zhang, G. J., and N. A. McFarlane, 1995: Sensitivity of climate simulations to the parameterization of cumulus convection in the Canadian Climate Centre general circulation model. *Atmos.–Ocean*, **33**, 407–446, https://doi.org/10.1080/07055900.1995.9649539.

Zhao, M., I. M. Held, and S. Lin, 2012: Some counterintuitive dependencies of tropical cyclone frequency on parameters in a GCM. *J. Atmos. Sci.*, **69**, 2272–2283, https://doi.org/10.1175/JAS-D-11-0238.1.